

Contents lists available at ScienceDirect

Colloids and Surfaces A: Physicochemical and Engineering Aspects

journal homepage: www.elsevier.com/locate/colsurfa



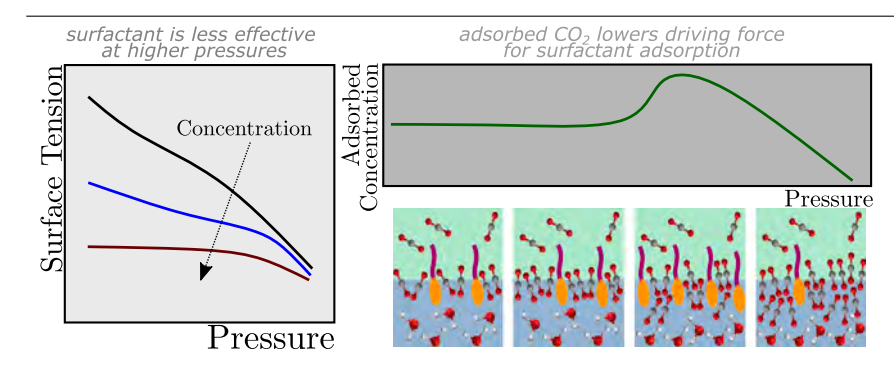


Pressure dependence of adsorption isotherm parameters and transport dynamics of a nonionic surfactant, LS-36, at the carbon dioxide (CO₂) gas–liquid water interface

Zachary R. Hinton, Emma Saloky, Nicolas J. Alvarez *

Drexel University, Department of Chemical and Biological Engineering, Philadelphia, PA 19104, United States of America

GRAPHICAL ABSTRACT



ARTICLE INFO

Keywords: Elevated-pressure surface tension Surfactant adsorption Carbon dioxide

ABSTRACT

Surfactants are important to a wide variety of elevated pressure processes; however, little is understood about the effect of pressure on surfactant interfacial thermodynamics or transport. While some experimental studies exist, concrete conclusions are difficult to infer due to experimental artifacts, e.g., non-equilibrium conditions. We recently showed that few experiments are capable of achieving bulk fluid saturation, which is essential to careful measurements of surfactant thermodynamics and transport dynamics. In other words, the accurate study of surfactant adsorption equilibrium and transport parameters first and foremost requires bulk fluids that are otherwise in equilibrium. This work uses our recently developed high pressure microtensiometer (HPMT), which ensures bulk phase saturation, to measure thermodynamic isotherms for tri(ethylene glycol)hexa(propylene glycol)-monododecyl ether (LS-36) surfactant (concentrations between 10⁻⁷ and 10⁻³ mol/L and pressures between 1 and 57 bar) at the CO2 gas-liquid water surface. All measurements were conducted at 22.5 $^{\circ}$ C. Note that in this study, the surfactant was dissolved in the liquid water phase and is unable to partition into the gaseous CO2 phase. Isotherms at different pressures were determined from surface tension data, analyzed, and compared to determine trends in thermodynamic parameters. Dynamic surface tension measurements were performed to assess transport dynamics in terms of the well-studied diffusion timescale. We find that surface tension depends non-linearly on pressure and surfactant concentration, such that surfactants are less effective at lowering surface tension as pressure increases. Furthermore, surfactant adsorption is a nonmonotonic function of pressure and goes through a maximum at intermediate pressures. This result suggests that surfactant adsorption is strongly dependent on the free energy of the CO2-water surface. Overall, this work shows that the thermodynamics of surfactants at equilibrium surfaces under pressure are non-trivial and need additional investigation to quantify the driving forces for surfactant adsorption and to develop models for high pressure processes.

E-mail address: nja49@drexel.edu (N.J. Alvarez).

Corresponding author.

1. Introduction

Surfactants are routinely used in high pressure applications, such as in detergency [1–5], in extraction and enhanced oil recovery [6–10], in polymer processing [11–15], in nano-material engineering [16,17], and as colloidal stabilizers [18,19]. The effect of pressure on the fundamental performance of surfactants is largely unknown and is often unaccounted for in the engineering of these systems. While theories relating surface tension to changes in pressure have been derived [20–25] and modeled computationally [26–30,30], experimental validation is lacking, especially in the case of surfactant solutions.

Measurements of pure fluid–fluid interfaces as a function of pressure are among the most common in the literature. For the organic liquid-water interface, interfacial tension (γ) is typically a simple function of pressure, whereby γ increases with increasing pressure [31,31–37]. For gas–water surfaces, γ is generally a more complex, decreasing function of pressure [33,38–44]. Overall, the gas–water surface is far more dependent on pressure than any other and is highly dependent on the gas phase chemistry. In a recent work [45], we demonstrated this principle for the gaseous CO_2 -water surface, whereby changes in CO_2 density, solubility, and adsorption lead to non-linear dependence of γ on pressure. This non-linearity has been attributed to a complex dependence of absorbed gas concentration with pressure, which translates to higher surface excess of CO_2 at the water–gas surface. The complex relationship of the clean surface tension on pressure further presses the need to understand how surfactants behave at these high pressure surfaces.

Several studies have measured the thermodynamics of surfactants at elevated pressure, such as surfactants at the water-oil interface [46-49], water-supercritical fluid interface [50–55], and the water-CO₂ (liquid) interface [50,51,56-61]. The water-CO₂ (liquid) interface is particularly interesting for its relevance to a wide variety of applications; however, there is still little understanding of how pressure changes surfactant adsorption behavior. Even fewer studies exist that examine the effect of pressure on surfactant adsorption at the watergas surface. A few examples at the water-gaseous CO₂ surface include: sodium chloride [62], tetra-n-butylammonium bromide [62], Tween 80 (polysorbate) [58], dipalmitoyl phosphatidylcholine [63], and fluorinated aerosol-OT and fatty alcohols in a Nickel plating solution [64]. Figure S1 summarizes the surface pressure as a function of pressure for the literature cited above and shows a general decrease in the surface tension with increasing pressure. One major, important fact is that there is no obvious relationship between the surface tension, equation of state, or overall surfactant behavior measured at ambient conditions, and that measured at elevated pressures.

Although there is a wide range of surfactants that are useful in elevated pressure processes, in this work we have chosen a surfactant with wide relevance to both theory and application. LS surfactants represent a family of amphiphile consisting of poly-glycol mono alkyl ethers where the hydrophilic poly-glycol (or head group) is a block copolymer of ethylene glycol (E_i) and propylene glycol (P_k). The structure follows $C_i E_j P_k$, where the naming convention is LS-(j)(k), i.e. LS-36 contains approximately three ethylene glycol units and six propylene glycol units, and hydrophobic tail is on average 12 carbons long (i.e. i =12) [65,66]. Block co-polymers of poly-glycols are well known for their versatility in a variety of solvents both as surfactants as well as bulk fluid modifiers; however, poloxamers are more typically considered over their alkyl ether analogs [67]. Some examples of applications for LS surfactants include in micellar catalysis [68], as detergents [69–71], and in chemical separations and extraction [72-74]. Recent interest in LS surfactants has increased, particularly as CO₂-philic surfactants are sought after for elevated pressure processes. While the most promising CO2 soluble surfactants are typically fluorinated, highly branched hydrocarbons, or siloxanes [75-77], block co-polymers of poly-glycols have proven to be similarly effective with lower associated cost and toxicity [51,59,65]. Thus, LS surfactants have found use in micellar

 CO_2 systems, particularly as solubilizers for organics [66,78] and water [65]. Fundamental experimental measurements of LS surfactant at the solution-vapor surface are relatively absent from the literature, with only two examples known for LS-45 and LS-54 [79,80] and one example for LS-36 at only high concentrations [81]. In this work, we examine LS-36 surfactant because it is both similar in chemistry to well-studied ethylene glycol surfactants [82] and is a known CO_2 -phile. Using this surfactant, we both report the fundamental nature of LS-36 adsorption and use this study to demonstrate model behavior of CO_2 -philic surfactants at the gaseous CO_2 surface, with hopes of future studies to assess dense CO_2 interfaces.

Recently we showed that thermodynamic equilibrium (i.e., phase saturation) between two fluid phases is very important to the state of the surface [45]. Furthermore, we showed that many measurement techniques detailed in the literature do not achieve equilibrium unless one waits extremely long times, much longer than reported in most studies, and longer than surfactant adsorption time scales. Thus, surfactant studies at elevated pressure using these methods do not study transport or equilibrium adsorption at an equilibrium interface, which makes thermodynamic evaluations difficult. In the aforementioned work, we described a novel high pressure microtensiometer (HPMT) that is capable of achieving thermodynamic equilibrium of the bulk phases prior to measuring surfactant adsorption dynamics and equilibrium [45].

In this work, we examine the adsorption of surfactants to the equilibrated CO2 vapor-solution surface as a function of pressure. We first demonstrate the independence of ambient surface tension of LS-36 surfactant solutions on the gas species and highlight the dependence of adsorption isotherm parameters on surfactant hydrophile chemistry for ethylene/propylene glycol containing surfactants. We then present the CO₂-LS-36 solution surface tension as a function of pressure (between 1 to 57 bar) at 22.5 °C, as measured using the HPMT. Our results indicate that surfactant becomes less effective at lowering surface tension (compared to the value at atmospheric pressure) with increasing pressure and concentration. Using a Langmuir isotherm and interfacial dilation measurements, we confirmed the non-monotonic pressure dependence of the maximum adsorption concentration and characteristic concentration of LS-36. We also demonstrate the impact of pressure-dependent adsorption on surfactant transport to the surface. This work underlines the complexities of molecular thermodynamics (e.g., CO₂ solubility, surfactant solution properties) involved in the pressure dependence of interfacial phenomena and highlights the need for further investigation of elevated-pressure surfactant behavior.

2. Experimental methods

Elevated pressure surface tension measurements were made using a high pressure microtensiometer (HPMT), shown in Fig. 1. The HPMT is based on the microtensiometer described by Alvarez et al. [83] and is described in detail in Hinton and Alvarez [45]. The HPMT consists of a micro-capillary inside a pressure chamber, such that surfactant solution resides in the main chamber and a CO_2 vapor-solution surface is introduced and pinned at the capillary tip. Two high pressure optical windows allow the surface to be imaged using an objective and camera, such that the interfacial radius (r) is continuously monitored. The differential pressure (ΔP) between the micro-capillary and the main chamber is measured by a high-pressure transducer. The chamber pressure (P) is measured by a gauge transducer. Surface tension (γ) is calculated using the Laplace equation, such that $\gamma = \Delta P \cdot r/2$.

The experimental protocol was as follows. The pressure chamber was thoroughly cleaned with deionized (DI) water until the surface tension at ambient pressure was measured to be a constant $\sim 72~\rm mN/m$ at 22.5 °C for greater than 3000 s. For surfactant experiments, solutions were loaded into the empty chamber using a syringe pump. Due to the high surface area of the system, depletion of surfactant to the walls of tubing, valves, and the pressure chamber was significant, particularly

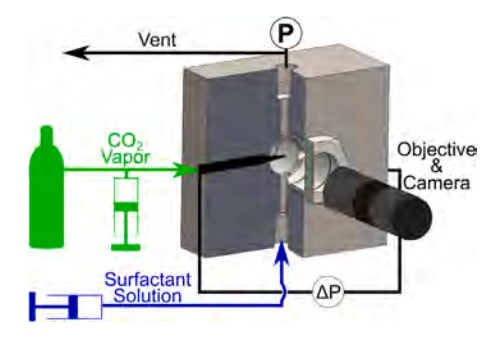


Fig. 1. Schematic of the HPMT experimental setup. A cutaway of the pressure chamber illustrates the position of the micro-capillary and introduction of CO_2 and surfactant solution into the HPMT. Only selected components are shown, with a more detailed description given in [45].

for dilute concentrations (see [84]). Therefore, surfactant solution was loaded to fill the system and allowed to sit for several hours before the depleted solution was exchanged with fresh solution. Using a surfactant solution of the desired concentration requires repeated applications of the same solution and long wait times. We have found it more advantageous and reproducible to instead allow the chamber walls to saturate several times from a slightly larger concentration of surfactant followed by filling with a slightly lower concentration of surfactant. This allows for rapid diffusion and adsorption of surfactant to the walls with an equilibrium reached such that the total bulk concentration is closer to the desired concentration, rather than severely depleted. The solution is allowed to equilibrate for > 12 hr after first being pressurized with CO_2 to ~ 50 bar and then open to the atmosphere. This ensures equilibrium of bulk surfactant with surfactant adsorbed to the walls and saturation of the surfactant solution with CO₂. A few repeated pressurization-depressurization cycles (between atmospheric pressure and 10 bar) were performed prior to measurements to ensure any excess dissolved gas or bubbles were removed from solution. We found that 5-10 repeated cycles was sufficient to obtain a stable pressure reading and reproducible surface tension results. The bulk concentration is then validated using the measured equilibrium surface tension at atmospheric pressure, by comparison to the 'calibration' isotherm measured in an ambient microtensiometer.

After the solution concentration reaches equilibrium with the cell walls, experiments begin at atmospheric pressure and are conducted with the chamber open. For elevated pressures, the chamber is closed and CO_2 is flowed through the capillary allowing for quick saturation of the solution and pressure to reach the desired set point [45]. A slight overshoot in pressure was often first reached, as venting removed any bubbles pinned to the cell walls. Dynamics were measured for surfaces starting at the point where a fresh surface is pinned to the capillary tip. Because of the relatively constant capillary pressure and changing surface tension, the bubble radius is dynamic during the measurement; however, for cases where the surface tension is reduced significantly throughout the experiment, the radius changes are too large to maintain a single surface. This was compensated for using the high pressure syringe pump by making small changes in the bubble fluid volume, maintaining a practically constant radius with small changes in the bubble pressure over time. After the surface tension remains constant for at least 100 s, the equilibrium surface tension, $\gamma_{eq},$ was recorded for at least 100 time points, where γ_{eq} is taken as the average of measurements at these time points. Note that all results are reported with error bars using a 95% confidence interval. This procedure is repeated for at least three surfaces for every measured pressure and concentration. The subsequent concentrations of surfactant are loaded using the same procedure, without rinsing between concentrations. All equilibration and measurement steps were performed at room temperature, i.e., 22.5 °C.

HPMT measurements of γ_{eq} were found to exhibit good reproducibility. Figure S2 illustrates example measurements in the form of individual replicates for two separate series of measurements. The precision of replicates at a given pressure is found to be very good; however, in some cases the accuracy between measurements is as high as ±2.5 mN/m. One likely reason for this variation in surface tension is that measurements were not taken at sufficiently long times. For industrial grade surfactants, artifacts of the impurities often cause a slow approach of equilibrium after the initial decrease in surface tension. This makes the interpretation of γ_{eq} difficult for multiple measurements, but in this work every effort is taken to consistently define γ_{eq} as the point where $\gamma(t)$ changes less than 1 mN/m over a period of at least 100 s. For decreasing pressure measurements, a lower degree of precision between measurements is observed. We hypothesize that this is due to nucleation of CO2 bubbles in the tubing of the HPMT during depressurization, leading to artifacts in the differential pressure measurement. For this reason, measurements performed after a depressurization were only performed after small pressure cycles to degas the system components.

While we acknowledge that our procedure is unconventional, it allows for the quickest, most reproducible data to be measured. Furthermore, there are clear advantages to our protocol over previously published examples. First, the saturation of the bulk solution with CO2 is of critical importance to studying true equilibrium surfaces. As discussed in our previous work [45], techniques commonly used in the literature (e.g., capillary rise, pendant drop) make saturation on experimentally-viable timescales difficult to ensure and require accurate density measurements to calculate surface tension. Whereas surfactant solutions are likely to complicate the accuracy of typical techniques, the HPMT achieves equilibrium quickly without requiring density measurements. Our careful attention to equilibration of the surfactant solution also addresses depletion effects, which are often neglected from the literature [84]. For high pressure instruments, this is particularly important because the volumes of instrumentation required to achieve elevated pressure are more likely to deplete solutions than ambient equipment. Moreover, depletion effects caused by surfactant solutions confined to a pendant drop can lead to inaccuracies in transport timescales and equilibrium surface tensions [85]. Thus, the HPMT considers saturation and equilibration of the surfactant solution as part of the experimental protocol to ensure measurements are subject only to equilibrium interfacial phenomena and not dynamic processes of bulk fluid equilibration. It should be noted that measurements at the solution-CO₂ liquid interface (or indeed other compressed liquids) could be performed using the same experimental apparatus; however, modifications to the protocol would be required to account for the potentially non-negligible solubility of water and surfactant in the dense CO₂ phase. This scenario should be the subject of future investigations.

2.1. Ambient measurements

Ambient measurements of surface tension are performed using the method and experimental setup described previously [86]. Briefly, a glass micro-capillary is embedded into a 3D-printed housing with a glass window at the bottom. The assembly is positioned on an inverted microscope and controlled, compressed gas is connected to the capillary, where gauge pressure inside the needle is measured. A well in the housing is filled with surfactant solution, and surfaces are pinned to the capillary tip at the beginning of a measurement. Surface tension is calculated using the Laplace equation discussed above. For dynamic measurements, the pressure at the capillary tip is exponentially reduced (using the microfluidics controller) such that the bubble remains pinned and its radius remains constant. Further details can be found in our previous works [83,86,87].

A series of concentrations between 1×10^{-7} and 1×10^{-3} mol/L of LS-36 were measured, obtaining both dynamic and equilibrium surface tensions. Note that for ambient measurements, the solutions were used

as prepared and depletion effects were avoided by allowing the solution to soak the cell for up to several hours and replacing with fresh solution prior to measurement. Measurements were made at the CO₂-water surface (using a compressed CO₂ feed to the controller) as well as at the air–water surface. At least 3 surfaces were measured for the reported averages. All measurements were made at room temperature (22.5 °C).

2.2. Materials

Surfactant solutions were made with DI water (18.2 M Ω cm) and LS-36 (Dehypon® LS 36, *BASF Corp.*, Florham Park, NJ) technical grade surfactant. The surfactant was used as received, i.e., without purification. Serial dilution was performed to ensure consistency across the entire concentration range. Compressed carbon dioxide and air (research grade) were obtained from *Airgas* (Radnor, PA) and used as received.

3. Results and discussion

3.1. Ambient dependence on gas phase

We start by measuring surface tensions for LS-36 at the ambient airwater and CO2-water surfaces as a function of concentration. Various works in the literature have shown that there is little to no difference between the surface tension measured at the water-air or water-CO₂ surface at ambient pressure [62,88]. This is confirmed by our additional measurements of ambient surface tension at the air-solution surface, shown in Figure S2a. Fit values of the Langmuir isotherm parameters Γ_{∞} and a, obtained by least-squares analysis, are in good agreement between air and CO2. Some disagreement arises from the lowest concentration data (i.e., surfactant bulk concentration, C_{∞} , < 10^{-6} mol/L), which occurs because of the very long timescales required to reach equilibrium that make determination of the 'true' γ_{eq} experimentally difficult for technical grade surfactants. Further comparison of the ratio of the surface tension for CO2 and air as a function of surfactant concentration is shown in Figure S3b, which shows that the data are equivalent within experimental error. From our understanding of the role of gas on the surface tension of water as a function of pressure [45], we expect that ambient surface tension is independent of whether CO2, N2, or air is used for the gas phase because of low solubility and minimal adsorption of all three gasses. Note this would not be the case for highly soluble gases, vapor phase adsorbates, or volatile surfactants [89-91].

The measured γ_{eq} at the CO₂-solution surface are shown in Fig. 2a with example dynamic surface tension given in Fig. 2b. Note that the molar concentrations are reported as calculated using the theoretical chemical structure, with a molar mass $M_W=666.97$ g/mol. The effect of polydispersity and technical purity is evident by both the behavior of $\gamma(t)$ at long times and the non-zero slope of γ_{eq} v. C_{∞} past the apparent critical micelle concentration (C_{CMC}). For this work, C_{CMC} was determined as the inflection point of γ_{eq} v. C_{∞} . The Langmuir-von Szyszkowski equation of state was fit to γ_{eq} versus C_{∞} below the C_{CMC} in the form:

$$\gamma_{eq} = \gamma_0 - RT \Gamma_{\infty} \ln \left(1 + \frac{C_{\infty}}{a} \right) \tag{1}$$

where γ_{eq} and γ_0 are the equilibrium and 'clean' surface tension, respectively, R is the gas constant, T is the temperature, Γ_{∞} is the maximum interfacial concentration of the surfactant, C_{∞} is the bulk surfactant concentration, and a is the surfactant characteristic concentration. The resulting fit parameters, are given in Table 1. While more robust adsorption isotherms may be preferred, the Langmuir EOS was used to minimize the number of parameters, facilitating analysis of the pressurized surface as discussed below. Our isotherm at high C_{∞} is in good agreement with published surface tensions for C_{∞} that are in the vicinity of C_{CMC} [81].

Table 1

Ambient isotherm parameters for LS surfactants.

Isotherm parameter	LS-36 ^a	LS-54 ^b	LS-45 ^b
$\Gamma_{\infty} (\text{mol/m}^2)$	1.72×10^{-6}	3.31×10^{-6}	1.50×10^{-6}
$a \text{ (mol/m}^3)$	3.29×10^{-6}	1.48×10^{-4}	5.29×10^{-7}
C_{CMC} (mol/L)	1.6×10^{-5}	2.51×10^{-5}	2.00×10^{-5}

- ^a Measured at the CO₂-water surface.
- $^{\rm b}$ Isotherm values obtained by non-linear, least squares fitting of Eq. (1) to digitized literature data from Refs. [79,80] for $C_\infty>10^{-6}$ mol/L.

Comparison of the ambient surface tension of LS-36 with other LS surfactant data available in the literature provides additional insight into the role of the hydrophile composition on interfacial quantities. Interestingly, the available surface tension data from the literature and the current work represent LS surfactants of equal hydrophile and hydrophobe lengths, i.e. for LS-36, LS-54 [80], and LS-45 [79] the hydrophobic tail length and the sum total of ethylene glycol and propylene glycol units are constant. Table 1 compares isotherm parameters measured in this work with those fit to literature data for LS-54 and LS-45. C_{CMC} for all three LS surfactants is similar, as is the value of surface tension beyond the C_{CMC} (not shown in table, approximately 30 mN/m). This is due to the dominance of the number of carbons in the hydrophobe on the C_{CMC} where the contribution of the hydrophile is negligible [82]. A more significant difference can be seen in the value of Γ_{∞} , or the slope of γ_{eq} versus $\log C_{\infty}$. Γ_{∞} is approximately the same for LS-36 and LS-45, however that of LS-54 is approximately a factor of 2 larger. This is indicative of the dependence of Γ_{∞} on the total hydrophobic content of the surfactant [82], which is clearly increased by the presence of a larger number of hydrophobic propylene glycol units (specifically, the additional pendant methyl groups). Furthermore, this effect is larger than expected for ethylene glycol only surfactants [82], likely due to the strong repulsive forces between adjacent propylene glycol groups at the surface. The order of magnitude difference in a values may signify the effect of the ratio of EO and PO groups on packing; however, no clear trend is observed. Note that experimental artifacts may also explain these results (i.e., values of a are difficult to accurately quantify without data at sufficiently low C_{∞} or appropriate accounting of depletion effects [82,84,92]). The relationships between isotherm parameters and LS surfactant structure have been discussed previously [93,94].

3.2. Pressure dependence of surfactant surface tensions

Fig. 3 shows the measured surface tension quantities as a function of pressure for varied concentration of LS-36 surfactant. The equilibrium surface tension, γ_{eq} , in Fig. 3a shows a decreasing trend with increasing pressure. The overall span of surface tension over the range of pressures is highest for the pure water surface and decreases as C_{∞} increases. Furthermore, the span of surface tension achievable at a given pressure decreases with increasing pressure, indicating that the role of surfactants is less pronounced at the surface as pressure increases. This finding reflects the behavior exhibited by many surfactants at the dense CO_2 -solution interface whereby surfactants often have little effect on γ_{eq} (see Figure S1). An alternative representation, i.e. the surface pressure, $\Pi = \gamma_0(P) - \gamma(C_{\infty}, P)$, is given in Figure S4, which indicates the effective lowering of surface tension with respect to the clean surface at the same pressure. For the majority of concentrations, this behavior appears to be non-monotonic with pressure, exhibiting a local maximum around P =40 bar, which is likely due to the onset of complex adsorption of CO₂ at the surface [45] leading to changes in the adsorption of surfactants (see discussion below). These data suggest that a targeted surface tension lowering can be achieved by manipulating either concentration of surfactant or pressure of the system.

Fig. 3b presents the surface tension lowering with respect to atmospheric pressure, i.e., $\gamma_{eq}^{atm} - \gamma_{eq}$. The largest value of this parameter is

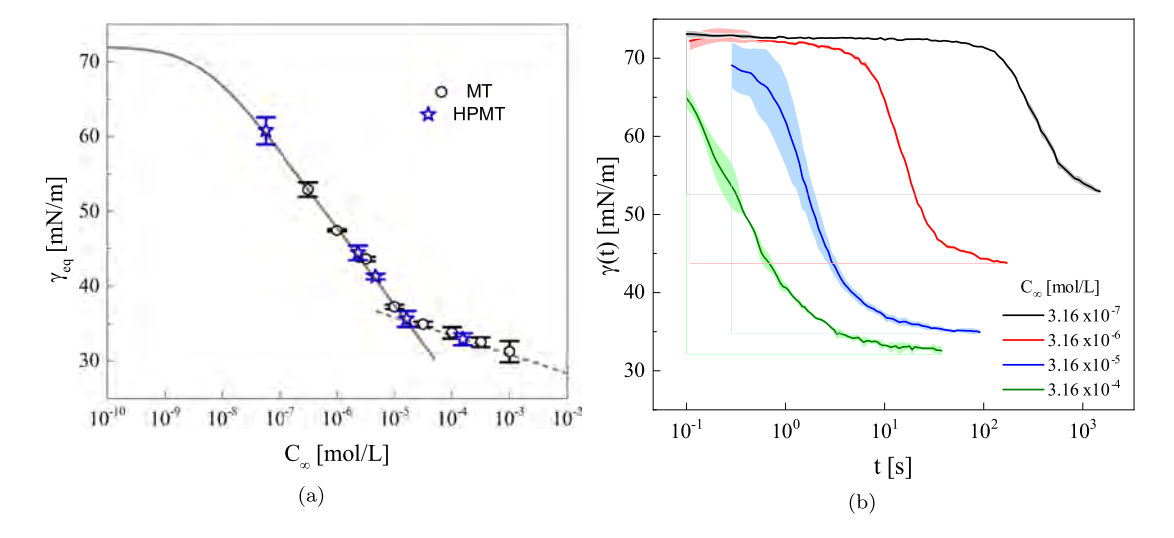


Fig. 2. Equilibrium (a) and example dynamic (b) surface tensions of LS-36 measured at the ambient CO_2 -water surface (i.e., using the ambient microtensiometer, MT) at different bulk surfactant concentrations (C_{∞}). In (a), error bars for equilibrium values represent 95% confidence intervals on the mean and the solid line represents the Langmuir equation of state fit to the data. The dashed line represents the approximate slope of γ_{eq} past the apparent C_{CMC} . The star symbols represent the ambient surface tensions measured using the HPMT. Dynamics were measured using an ambient microtensiometer. Lines represent average values between 3 experiments and shaded regions represent one standard deviation away from the mean.

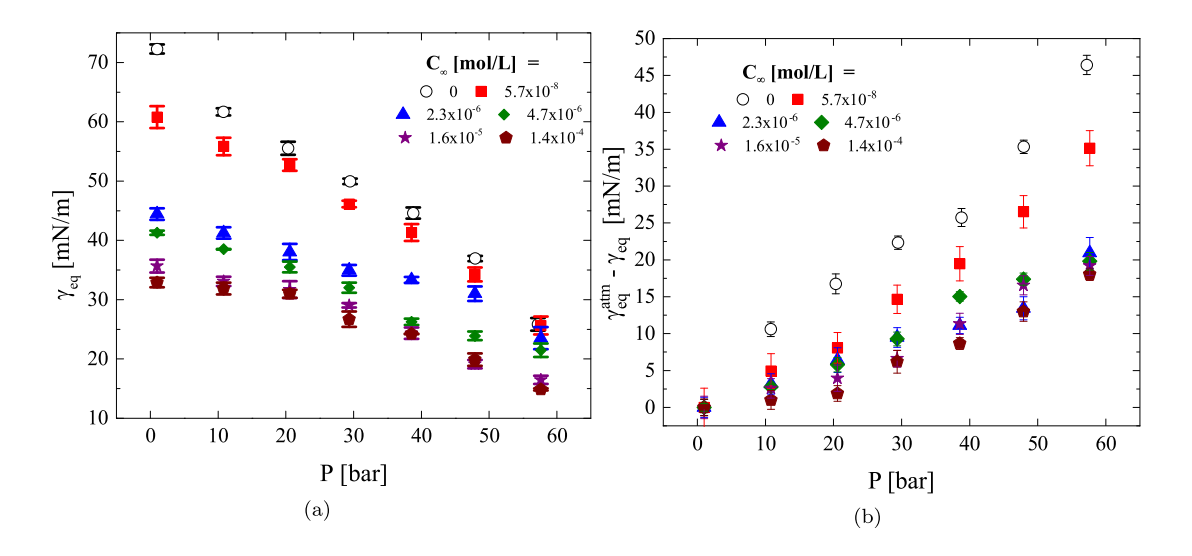


Fig. 3. Surface tension (a) and difference from ambient surface tension (b) as a function of pressure for LS-36 solutions. All measurements were made at 22.5 °C. Error bars represent propagated 95% confidence intervals using the errors of measured quantities (i.e., γ_0 , γ_{eq} , and γ_{eq}^{alm}).

observed for the clean CO_2 -water surface and decreases with increasing surfactant concentration. This suggests that adsorbed CO_2 is more effective at reducing surface tension than surfactant, which would not be obvious from previous studies where surfactant likely adsorbs to a non-equilibrium surface [45]. This implies that the 'effectiveness' of the surfactant is low at higher pressures because the surface free energy is sufficiently lowered by adsorbed (surface excess) CO_2 . Because the HPMT ensures an equilibrium clean surface prior to surfactant adsorption, it is likely that CO_2 both thermodynamically and sterically hinders adsorption of surfactant.

This behavior is similar to that observed by Massoudi and King whereby increasing concentrations of TBAB lowered the change in surface tension compared to that measured at ambient pressure ($\gamma_{eq}^{atm} - \gamma_{eq}$) [62]. The authors hypothesized that the surface at elevated pressure is composed of more CO₂ than surfactants and that surfactant

undergoes a change in hydrophobic interactions at the surface because of adsorbed gas; however, in the case of hydrophobic gases, the opposite trend was observed. The authors did not consider the effect of dissolved gasses, but it is expected that CO_2 dissolution, however small, would be much greater than that of hydrophobic gasses and would also change the solution chemistry such that charged surfactants like TBAB must undergo some change in solution and at the surface. For our system of LS-36, it can be expected that changes in the hydrophobic interactions at the surface could be due to changes in hydration and the structure of water surrounding surfactant molecules. In particular, this is known to be prominent in propylene glycol containing surfactants [95]. These effects combined with pressure driven changes to the density and adsorption of CO_2 lead to complex interactions and evaluation of surface tensions.

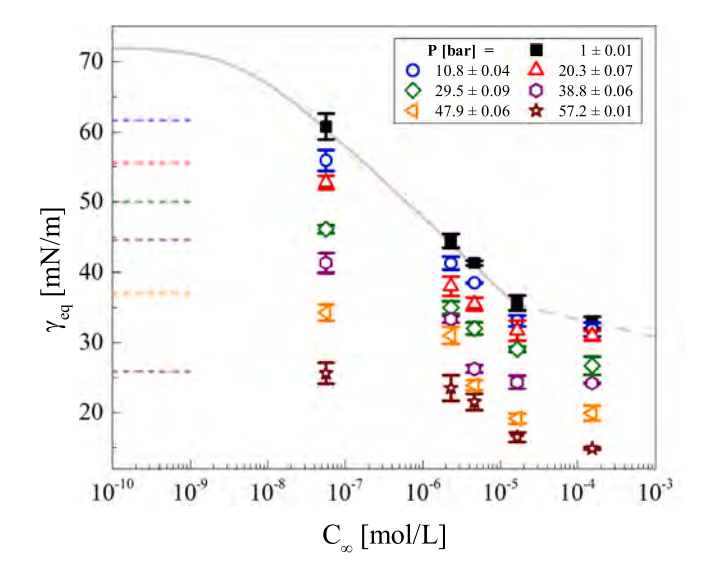


Fig. 4. Surface tension isotherms at selected pressures. Error bars represent 95% confidence intervals. The isotherm and post- C_{CMC} slope is shown for atmospheric pressure. Dashed lines represent γ_0 at each pressure. Pressures given in the legend represent the mean chamber pressure for all concentrations with 95% confidence intervals representing the distribution.

3.3. Pressure dependence of the equation of state

The interfacial adsorption of surfactant is quantified in terms of an isotherm/equation of state, i.e., γ_{eq} versus C_{∞} , for varying pressures. This analysis provides a useful comparison of the effect of elevated pressure on the fundamental properties of the surfactant. Fig. 4 shows the equilibrium surface tension as a function of surfactant concentration for a range of pressures. Note that experimentally, measurements are made at fixed C_{∞} and varying P, which results in a slight variability in pressure that is denoted by the error indicated in the legend. The effect of pressure on the isotherms appears to be twofold: (i) a decrease in the overall change in surface tension with increasing pressure and (ii) a change in the shape of the isotherm with increasing pressure. The change in the magnitude of the isotherm appears as a decrease in the slope for certain pressures and an increase in the proximity of γ_{eq} to γ_0 at low concentration for increasing pressure, i.e. a decrease in Π with increasing pressure. This occurs because of changes in γ_0 due to pressure, as well as changes in the adsorption of surfactant. The fact that Π versus C_{∞} (shown in Figure S5) does not collapse for any pressures indicates a fundamental change in the isotherm, i.e. the isotherm is not simply shifted by a change in γ_0 . While this finding agrees with the results of Massoudi and King, the dependence of Π on C_{∞} is significantly larger for this study [62]. This difference may be related to the much greater surface activity of LS-36 over the tetran-butylammonium bromide (TBAB) used by Massoudi and King, or it may be linked to the fact that the bulk fluids are at thermodynamic equilibrium in this study [45]. The effect of pressure on the adsorption isotherm can be quantified by fitting a model to the data to obtain isotherm parameters and C_{CMC} .

3.3.1. Effect of pressure on adsorption

In our previous work, we showed that the pressure dependent adsorption of CO_2 is complex, especially for P > 30 bar, and follows a van der Waals pressure isotherm [45]. For surfactant solutions, typically the Langmuir, Frumkin, or generalized Frumkin isotherms are applied [96]. For moderate pressures where the shape of the isotherm is not significantly different than the ambient isotherm, the Langmuir equation of state from Eq. (1) was fit using least squares regression with results shown in Figure S6a. Although pressure-induced changes to the surface

(e.g., hydrogen bonding, surfactant hydration) are likely to invalidate some of the assumptions of the Langmuir isotherm [96], we have chosen to use this isotherm for its simplicity. The Langmuir isotherm is the simplest non-linear model (containing only two parameters) to fit to surface tension data and the interpretation of its parameters facilitates comparison of surfactant phenomena within a well understood context. However, future work should consider more complicated adsorption isotherms. The data in this work are well described by the isotherm for moderate pressures; however, this is not the case for higher pressure data (confirming the need for more descriptive models). Rather, the maximum adsorption concentration, Γ_{∞} was estimated using the slope of the data and the Gibbs equation of state, given by

$$\Gamma = -\frac{1}{RT} \left(\frac{d\gamma}{d \ln C_{\infty}} \right) \approx -\frac{1}{RT} \frac{\Delta \gamma}{\Delta \ln C_{\infty}}$$
 (2)

The slope of the data was approximated by the derivative between adjacent experimental data points, which approximates \varGamma at the midpoint C_∞ in log-scale. We define this adsorption excess as \varGamma_{ap} . For sufficiently high concentration of surfactant, this value is expected to approach \varGamma_∞ . For this analysis, we assume that the Gibbs equation is applicable, i.e., the solution activity coefficient approaches unity (dilute solution) and γ versus $\ln C_\infty$ is linear $(C_\infty \to C_{CMC})$ [92]. These assumptions appear relatively consistent with standard approaches [92] and the shape of the measured isotherms. While this method may be applied to any two data points, we chose $C_\infty \approx 3.3 \times 10^{-6}$ mol/L. The results of this analysis are shown in Fig. 5a, where the values obtained from the Langmuir best-fit and the Gibbs isotherm are in good agreement. This further validates the values of γ_{ea} measured.

For larger pressures, an additional approach of rapid surface compression measurements was used to determine the maximum surface concentration. These measurements consist of a rapid change in the area of the bubble's surface, such that the corresponding change in surface tension relates to the adsorbed concentration at the initial and final area by means of the isotherm. Measurements are performed by quick changes in the volume of the syringe pump, which causes the surface to dilate while remaining pinned to the tip of the capillary. The advantage to this method is its independence from errors in the isotherm data because it is performed at only a single concentration. This method also serves as an independent confirmation of the Γ_{∞} for the same reason. Figure S6b illustrates typical compression measurements, where before the compression, $t < t_0$, the surface is at equilibrium with the bulk and γ_{eq} is measured. The surface is quickly compressed with a small change in area and the measured surface tension immediately after the area change is decreased due to a larger, non-equilibrium interfacial concentration. The surface then reverts to equilibrium, via diffusion to the bulk, returning to γ_{eq} . In all experiments, we observe the eventual return of the surface tension to its equilibrium value, confirming that the surfactant is reversibly adsorbed.

The instantaneous change in measured surface tension, which is highlighted in the box and inset of Figure S6b, is used to quantify the equilibrium adsorption at the surface through a given adsorption model. Assuming Langmuir adsorption, the surface equation of state can be written in terms of the number of moles of surfactant at the surface, n:

$$\gamma = \gamma_0 + RT \Gamma_{\infty} \ln \left(1 - \frac{n}{\Gamma_{\infty} A} \right) \tag{3}$$

where A is the interfacial area [97]. We again assume a Langmuir adsorption isotherm and that the compression or expansion is rapid enough such that the adsorbed moles of surfactant are constant. Thus the mole balance gives,

$$n(A_1) = n(A_2) = A_i \ \Gamma_{\infty} \left[1 - \exp\left(\frac{\gamma_i - \gamma_0}{RT\Gamma_{\infty}}\right) \right]$$
 (4)

where A_i and γ_i represent the surface area and measured surface tension at times immediately before and after the surface dilation. For

a toroidal spherical cap smaller than hemispherical, the surface area is given by:

$$A = 2\pi r \left(r - \sqrt{r^2 - b^2} \right) \tag{5}$$

where b is the capillary radius. Thus for a given change in radius and surface tension measured for a dilating interface, Γ_{∞} is determined from the mole balance (4). Note that this only holds for the step change in area, i.e. typically < 2 s, where mass transfer is negligible, reversible adsorption, and for small perturbations to the interfacial area (i.e., small dilatational strains) [97]. Using Γ_{∞} estimated from interfacial expansion, the corresponding value of a can be evaluated from a rearrangement of the Langmuir isotherm,

$$\frac{\Gamma}{\Gamma_{\infty}} = \frac{n}{A_1 \Gamma_{\infty}} = \frac{C_{\infty}}{C_{\infty} + a} \tag{6}$$

where C_{∞} is the bulk concentration at the equilibrium adsorption concentration. Therefore an expansion/compression measurement at a single concentration provides a relatively accurate estimation of the Langmuir isotherm for all concentrations.

The results of the isotherm fitting (Γ_{∞} and a, i.e., from Eq. (1)), slope estimation (Γ_{ap} , i.e., from Eq. (2)), and rapid compression measurements ($\Gamma_{\infty,ap}$ and a_{ap} , i.e., from Eqs. (4)-(6)) are shown in Fig. 5. We first note that the agreement between the various methods of obtaining Γ and a is satisfactory, with less than 30% deviation between the various methods. Particularly, for $P \approx 20$ bar, where all three methods were applied, there is very good agreement between the results of the isotherm fit and the interfacial dilation in both Γ_{∞} and a. For $P \ge 40$ bar, the deviation in Γ_{∞} is the highest between the slope approximation and compression experiments. We hypothesize that this is due to the limitations of taking the derivative of so few experimental points at these values of P and C_{∞} . Regardless of the quantitative difference in Γ_{∞} for the two methods, the trends are consistent, and both methods show a maximum in surface coverage at intermediate pressure. A local maximum in Γ_{∞} is observed at around $P \approx 40$ bar, followed by a decrease of adsorption as a function of pressure, where Γ_{∞} at $P \approx 57$ bar is less than that at low pressures by about an order of magnitude. The value of a determined from the Langmuir isotherm is a very strong function of pressure, varying by almost an order of magnitude over less than 20 bar. A maximum is also observed for a at the same pressures discussed for Γ_{∞} . The free energy of adsorption is related to a by the relationship: $\Delta G^{ads} \sim RT \ln a$ [82], thus, the free energy of adsorption increases at an approximate rate of 1.5RT per 10 bar. An interesting fact is that the sharp increase and maximum in Γ_{∞} and a for $P \approx 40$ bar corresponds to the maximum in $\partial \gamma / \partial P$ and the onset of non-Langmurian (i.e., multilayer) adsorption for the pure water-CO2 surface [45]. This corresponding behavior alludes to a potential surfactant adsorption mechanism that is dependent upon both the surface excess concentration and interfacial structure of CO2. Our hypothesis is that the simply adsorbed CO₂ does not impede adsorption of surfactant, but that CO2 lowers the surface free energy enough that surfactant adsorption is less likely. Once more complex adsorption of CO2 occurs, a sudden need for surfactant to lower the surface free energy occurs, but this need dissipates because with increasing pressure more CO2 becomes available to adsorb instead of surfactant. Further experiments and modeling would be useful in understanding this connection further.

3.3.2. Effect of pressure on micellization

Further analysis of the isotherm data was performed to estimate C_{CMC} . The effects of the technical grade surfactant as well as the wide differences in C_{∞} make accurate determination of C_{CMC} difficult. Therefore, we estimate an apparent CMC, C_{CMC}^{ap} , from the intersection of the Langmuir isotherm and a line drawn between the surface tension of the two highest concentration data points. Additional details are discussed in the supplementary material. The values of C_{CMC}^{ap} as a function of pressure with corresponding error bars are shown in Fig. 6.

Fig. 6 shows a slight decrease in C_{CMC}^{ap} with increasing pressure up to $P \approx 40$ bar after which an increase is observed. As expected, the trend of C_{CMC} inversely follows the trends observed in both Γ_{∞} and a. Unfortunately, the number of data points used for 57 bar do not provide sufficient certainty in the value of CMC, and therefore further work is needed to confirm the non-monotonicity with pressure. From the data in Figs. 5b and 6, it is clear that the difference between the free energies of micellization and adsorption, $\Delta G^{mic} - \Delta G^{ads} \approx$ $RT \ln (C_{CMC}/a)$, decreases with pressure, suggesting surfactant becomes less likely to adsorb with increasing pressure, while the driving force for micellization remains relatively constant. At the maximum in Γ_{∞} around 40 bar, micellization and adsorption become equally likely, followed by increasing propensity for adsorption and a slight decrease in the propensity for micellization. This supports the idea that increased CO2 adsorption with increasing pressure at relatively low pressures, reduces the need for surfactant to lower surface free energy, increasing surfactant propensity for micellization. However, at elevated pressures and complex CO2 interfacial adsorption, surfactant adsorption spikes and propensity for micellization decreases. Another factor to consider is the decreasing pH of water with increasing pressure (from 4.22 at 1 bar to 2.92 at 57 bar, based on correlation with CO₂ solubility [98]), which potentially contributes to changing CMC. Examples of the pH dependence of C_{CMC} have shown that differing trends can emerge depending on surfactant chemistry due to structural changes to water surrounding micelles, local dipole screening, and surfactant interactions [99–101]. More experiments, such as neutron scattering might help to better understand the effect of pressure on the micelle structure and size, particularly as a function of pH.

These results are in contrast to several literature examples whereby the C_{CMC} was constant with increasing pressure or had a slight monotonic increase with pressure [47,102-105]. It is important to highlight that most literature examples measure the C_{CMC} either in the absence of a secondary phase using techniques such as spectroscopy or via interfacial tension at the oil-water interface [47,102-104]. One explanation for the trend in C^{ap}_{CMC} observed here is the effect of dissolved gas on the chemical potential. It is well known that solutes (regardless of surface activity) and temperature can cause a sometimes non-monotonic change in C_{CMC} for even nonionic surfactants because of fundamental changes in hydration and water structure surrounding a micelle [92]. In one of the few examples of the role of pressure driven dissolution of CO_2 on changing $C_{CMC},$ Chen et al. found a non-monotonic change in C_{CMC} with increasing pressure for AOT in iso-octane solutions [106]. This effect is attributed to increased thermodynamic favorability of micellization because of CO₂-surfactant interaction and changes in the hydrophobicity of the bulk solvent. Interestingly, the effect of CO₂ on our aqueous solutions is similar in magnitude to the previous study, even though CO2 is far less soluble in water and the LS-36 is nonionic. We hypothesize that this is because of the much lower starting hydrophilicity/polarity of LS-36, which is more strongly impacted by the presence of the polar dissolved CO₂ and carbonate ions. Carbonate ions in particular have shown to strongly impact the thermodynamics of propylene glycol containing surfactants [95]. Additionally, when considered in terms of changing pH one would also expect a nonmonotonic change in C_{CMC} due to changes in solvent structure and local dipole screening [99,100]. However, this remains only a hypothesis and cannot be confirmed without further study using additional techniques.

3.4. Dynamic surface tension

Lastly, we briefly discuss the dynamic surface tensions measured as a function of pressure. Elevated pressure dynamics are of great interest to a variety of surfactant transport processes; however, as discussed in our previous work, the vast majority of 'clean' water–CO₂ interfaces have been reported to undergo dynamics because of transport of CO₂

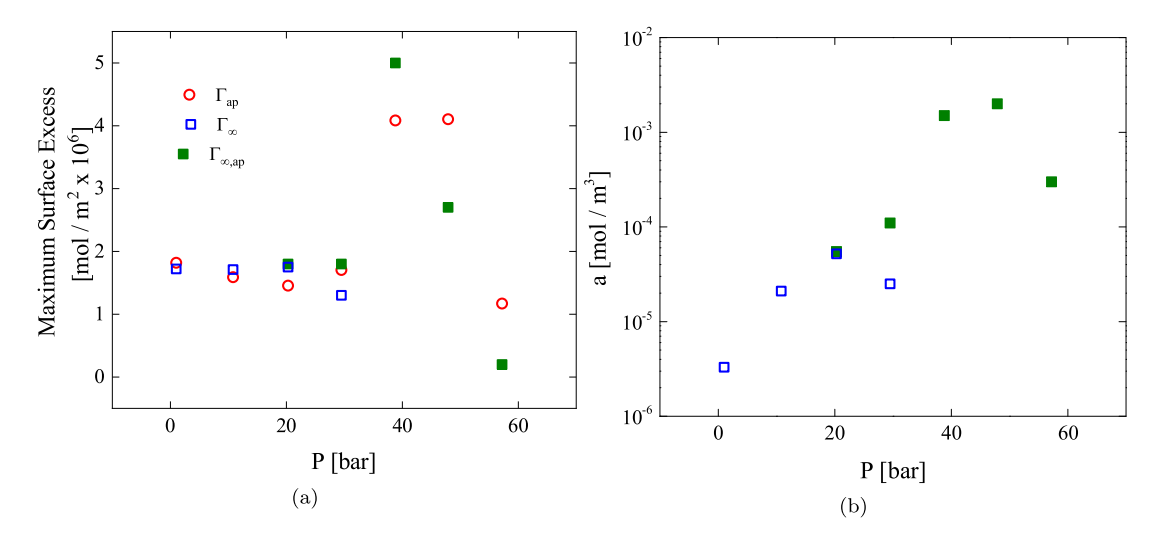


Fig. 5. (a) Values of the maximum surface excess concentration and (b) characteristic concentration, a, as a function of pressure. Open circles represent the apparent value, Γ_{ap} , obtained from the slope (Eq. (2)), $d\gamma_{eq}/d(\ln C_{\infty})$, at $C_{\infty}\approx 3.3\times 10^{-6}$ mol/L. Open squares represent values of Γ_{∞} and a obtained from fits of the Langmuir equation of state (Eq. (1)), as shown in Fig. 6a. Filled squares represent the apparent values of Γ_{∞} and a from rapid compression experiments (Eqs. (4)–(6)).

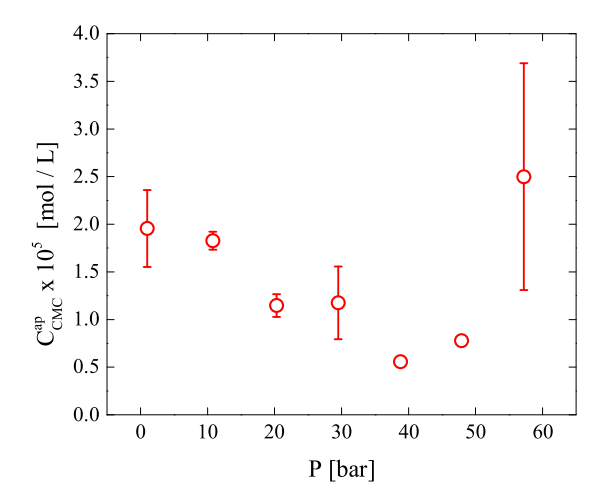


Fig. 6. Apparent critical micelle concentration, C^{qp}_{CMC} , as a function of pressure. Symbols represent the mean and error bars represent the approximate range, as detailed in the supplemental material.

in non-equilibrium conditions [45]. This suggests that previously reported surfactant dynamics at elevated pressure are obscured by $\rm CO_2$ transport occurring on longer or comparable timescales. In the case of the high pressure microtensiometer, dynamics are observed only after the surfactant solution is saturated with $\rm CO_2$, meaning the dynamics are directly comparable to typical surfactant transport phenomena.

Fig. 7a shows an example of dynamic surface tension at fixed C_{∞} and various pressures. In all cases, the surface tension begins at the clean surface tension value and then decreases to γ_{eq} . The shape of the dynamic curve is strongly dependent on the isotherm parameters. A simple timescale analysis was performed to determine the governing transport mechanism [107]. At ambient pressure, the transport of LS-36 is governed by diffusion (see dynamics in Fig. 2b). This is demonstrated in Fig. 7b, where the experimental timescale is approximately equal to the diffusion timescale for all C_{∞} , as detailed in Alvarez et al. [108].

For elevated pressures, the experimental timescale can only be affected by either changes in Γ_{eq} , a, or the diffusion coefficient, D. Changes in D are expected to be negligible because of the limited change in water's viscosity [109] as a function of pressure. It is possible that dissolved CO_2 could have any impact on D; however, the effect is likely negligible. Thus, the value of $D=1\times 10^{-10}~\mathrm{m}^2/\mathrm{s}$, estimated from

typical values for surfactants of similar molecular weight and structure, is expected to hold for all pressures [108].

The diffusion timescale can be estimated from Alvarez et al. [108] considering the isotherm parameters discussed above. Fig. 7b shows the experimental transport timescales normalized by $\tau_{D,s}$ and shown as a function of pressure. For all measurements, the normalized timescale is near unity, which suggests that transport is governed by diffusion of surfactant molecules to the surface. Note that some spread of the data at various pressures is most likely due to experimental error such as convection inside the sample cell, and/or an initially unclean surface. Thus we can conclude that pressure has no appreciable affect on the rate of surfactant transport to the surface, but mostly affects the magnitude of the isotherm/surface equation of state parameters.

4. Conclusions

The control and refinement of high pressure chemical processes requires a fundamental understanding of the effect of pressure on interfacial thermodynamics [18,19]. Unfortunately there exist few studies that have accurately measured surfactant physics at elevated pressures [110]. This work shows the importance and non-monotonic dependence of interfacial thermodynamics on pressure. We present a thorough investigation of a commercially relevant surfactant, LS-36, to the pressurized and equilibrated CO2-solution interface using a novel HPMT. The equilibrium/saturation of the bulk phases allowed for the unique determination of key thermodynamic parameters as a function of pressure. It is worth noting that previous studies have often been hindered by unsaturated bulk fluids [45], which convoluted the effect of surfactants. We show that the interfacial thermodynamics of LS-36 are non-monotonic, and show a complicated function of pressure. Four major conclusions from this work are: (1) surfactants have a weaker effect on surface tension for increased pressure, (2) isotherm parameters Γ_{∞} and a go through a maximum at intermediate pressures, where the adsorption of CO2 molecules to the interface was previously shown to be complex, (3) the CMC for LS-36 goes through a minimum at intermediate pressures, and (4) adsorption for LS-36 is diffusion limited for all measured pressures. This technique can be readily extended to measurements of additional surfactants at various gas-liquid and liquid-liquid interfaces as a function of pressure. These measurements are the subject of future investigations and will help to better understand whether the above conclusions are specific to CO₂-water, or are more general effects of pressure on surfactant thermodynamic properties.

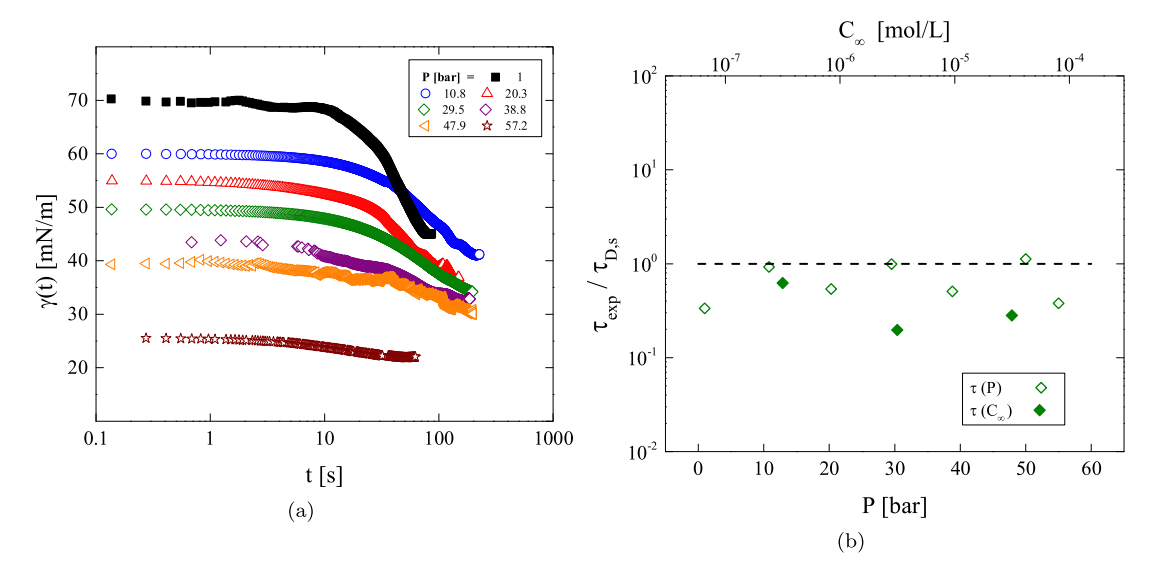


Fig. 7. (a) Dynamic surface tension for $C_{\infty} = 2.3 \times 10^{-6}$ mol/L at varying pressure. Note that dynamics are smoothed using a cubic Savitzky–Golay filter with $\sim 30\%$ windows. (b) Corresponding adsorption timescale to reach equilibrium normalized by the spherical diffusion timescale.

CRediT authorship contribution statement

Zachary R. Hinton: Data curation, Methodology, Formal analysis, Writing – original & editing. **Emma Saloky:** Methodology, Data curation, Formal analysis. **Nicolas J. Alvarez:** Methodology, Writing – review & editing, Supervision.

Declaration of competing interest

The authors declare that they have no known competing financial interests or personal relationships that could have appeared to influence the work reported in this paper.

Data availability

Data will be made available on request.

Acknowledgments

This work was supported by the National Science Foundation, United States under grant no. CBET-1847140.

Appendix A. Supplementary data

Supplementary material related to this article can be found online at https://doi.org/10.1016/j.colsurfa.2023.132767.

References

- S. Banerjee, S. Sutanto, J.M. Kleijn, M.J.E. Van Roosmalen, G.J. Witkamp, M.a.C. Stuart, Colloidal interactions in liquid CO 2 - A dry-cleaning perspective, Adv. Colloid Interface Sci. 175 (2012) 11–24, http://dx.doi.org/10.1016/j.cis. 2012.03.005.
- [2] M.J.E. Van Roosmalen, G.F. Woerlee, G.J. Witkamp, Amino acid based surfactants for dry-cleaning with high-pressure carbon dioxide, J. Supercrit. Fluids 32 (1–3) (2004) 243–254, http://dx.doi.org/10.1016/j.supflu.2004.01.005.
- [3] M.J.E. Van Roosmalen, G.F. Woerlee, G.J. Witkamp, Surfactants for particulate soil removal in dry-cleaning with high-pressure carbon dioxide, J. Supercrit. Fluids 30 (1) (2004) 97–109, http://dx.doi.org/10.1016/S0896-8446(03)00115-
- [4] N.M. Lawandy, A.Y. Smuk, Supercritical fluid cleaning of banknotes, Ind. Eng. Chem. Res. 53 (2) (2014) 530–540, http://dx.doi.org/10.1021/ie403307y.
- [5] J.a. Keagy, Y. Li, P.F. Green, K.P. Johnston, F. Weber, J.T. Rhoad, E.L. Busch, P.J. Wolf, CO2 promotes penetration and removal of aqueous hydrocarbon surfactant cleaning solutions and silylation in low-k dielectrics with 3 nm pores, J. Supercrit. Fluids 42 (3 SPEC. ISS.) (2007) 398–409, http://dx.doi.org/10.1016/j.supflu.2007.02.007.

- [6] M. Mazzotti, R. Pini, G. Storti, Enhanced coalbed methane recovery, J. Supercrit. Fluids 47 (3) (2009) 619–627, http://dx.doi.org/10.1016/j.supflu.2008.08. 013.
- [7] M. Blunt, F. Fayers, F.M. Orr, Carbon dioxide in enhanced oil recovery, Energy Convers. Manag. 34 (9–11) (1993) 1197–1204, http://dx.doi.org/10. 1016/0196-8904(93)90069-M.
- [8] a.M.F. Palavra, J.P. Coelho, J.G. Barroso, a.P. Rauter, J.M.N.a. Fareleira, a. Mainar, J.S. Urieta, B.P. Nobre, L. Gouveia, R.L. Mendes, J.M.S. Cabral, J.M. Novais, Supercritical carbon dioxide extraction of bioactive compounds from microalgae and volatile oils from aromatic plants, J. Supercrit. Fluids 60 (2011) 21–27, http://dx.doi.org/10.1016/j.supflu.2011.04.017.
- [9] E. Reverchon, R. Adami, S. Cardea, G.D. Porta, Supercritical fluids processing of polymers for pharmaceutical and medical applications, J. Supercrit. Fluids 47 (3) (2009) 484–492, http://dx.doi.org/10.1016/j.supflu.2008.10.001.
- [10] J. Porschmann, L. Blasberg, K. Mackenzie, P. Harting, Application of surfactants to the supercritical fluid extraction of nitroaromatic compounds from sediments1, J. Chromatogr. A 816 (2) (1998) 221–232, http://dx.doi.org/10.1016/S0021-9673(98)00467-1, URL http://linkinghub.elsevier.com/retrieve/pii/S0021967398004671.
- [11] B. Baradie, M.S. Shoichet, Z. Shen, M.a. McHugh, L. Hong, Y. Wang, J.K. Johnson, E.J. Beckman, R.M. Enick, Synthesis and solubility of linear poly(tetrafluoroethylene-co-vinyl acetate) in dense CO 2: Experimental and molecular modeling results, Macromolecules 37 (20) (2004) 7799–7807, http://dx.doi.org/10.1021/ma049384u.
- [12] J.M. Desimone, E.E. Maury, Y.Z. Menceloglu, J.B. McClain, T.J. Romack, J.R. Combes, Dispersion polymerizations in supercritical carbon dioxide, Science (80-.). 265 (5170) (1994) 356–359, http://dx.doi.org/10.1126/science.265. 5170.356.
- [13] C. Gutiérrez, J.F. Rodríguez, I. Gracia, a. De Lucas, M.T. García, Development of a strategy for the foaming of polystyrene dissolutions in scCO2, J. Supercrit. Fluids 76 (2013) 126–134, http://dx.doi.org/10.1016/j.supflu.2013.01.020.
- [14] I. Tsivintzelis, A.G. Angelopoulou, C. Panayiotou, Foaming of polymers with supercritical CO2: An experimental and theoretical study, Polymer (Guildf). 48 (20) (2007) 5928–5939, http://dx.doi.org/10.1016/j.polymer.2007.08.004.
- [15] M. Goto, Chemical recycling of plastics using sub- and supercritical fluids, J. Supercrit. Fluids 47 (3) (2009) 500–507, http://dx.doi.org/10.1016/j.supflu. 2008.10.011.
- [16] F. Cansell, C. Aymonier, Design of functional nanostructured materials using supercritical fluids, J. Supercrit. Fluids 47 (3) (2009) 508–516, http://dx.doi. org/10.1016/j.supflu.2008.10.002.
- [17] J.D. Holmes, D.M. Lyons, K.J. Ziegler, Supercritical fluid synthesis of metal and semiconductor nanomaterials, Chem. - A Eur. J. 9 (10) (2003) 2144–2150, http://dx.doi.org/10.1002/chem.200204521.
- [18] J. Eastoe, B.M.H. Cazelles, D.C. Steytler, J.D. Holmes, A.R. Pitt, T.J. Wear, R.K. Heenan, Water-in-CO 2 microemulsions studied by small-angle neutron scattering, Langmuir 13 (26) (1997) 6980–6984, http://dx.doi.org/10.1021/ la970876s, URL http://pubs.acs.org/doi/abs/10.1021/la970876s.
- [19] K.P. Johnston, S.R.P.D. Rocha, Colloids in supercritical fluids over the last 20 years and future directions, J. Supercrit. Fluids 47 (3) (2009) 523–530, http://dx.doi.org/10.1016/j.supflu.2008.10.024.
- [20] R.S. Hansen, Thermodynamics of interfaces between condensed phases, J. Phys. Chem. 66 (5) (1962) 410–415.

- [21] J. Eriksson, On the thermodynamic theory for the effect of pressure on surface tension, Acta Chem. Scand. 16 (1962) 2199–2211.
- [22] K. Motomura, H. Iyota, M. Aratono, M. Yamanaka, R. Matuura, Thermodynamic consideration of the pressure dependence of interfacial tension, J. Colloid Interface Sci. 93 (1) (1983) 264–269, http://dx.doi.org/10.1016/0021-9797(83) 90404-6
- [23] G.N. Lewis, M. Randall, Thermodynamics and the Free Energy of Chemical Substances, first ed., McGraw-Hill, New York, 1923.
- [24] L.A. Turkevich, J.A. Mann, Pressure dependence of the interfacial tension between fluid phases. 1. Formalism and application to simple fluids, Langmuir 6 (2) (1990) 445–456, http://dx.doi.org/10.1021/la00092a027.
- [25] A.I. Rusanov, V.A. Prokhorov, Interfacial Tensiometry, Elsevier, Amsterdam, 1996, http://dx.doi.org/10.1016/S1383-7303(96)80031-7.
- [26] A. Ghoufi, P. Malfreyt, D.J. Tildesley, Computer modelling of the surface tension of the gas-liquid and liquid-liquid interface, Chem. Soc. Rev. 45 (5) (2016) 1387–1409, http://dx.doi.org/10.1039/C5CS00736D, URL http://xlink.rsc.org/ ?DOI=C5CS00736D.
- [27] S. Becker, S. Werth, M. Horsch, K. Langenbach, H. Hasse, Interfacial tension and adsorption in the binary system ethanol and carbon dioxide: Experiments, molecular simulation and density gradient theory, Fluid Phase Equilib. 427 (2016) 476–487, http://dx.doi.org/10.1016/j.fluid.2016.08.007.
- [28] K.D. Papavasileiou, O.A. Moultos, I.G. Economou, Predictions of water/oil interfacial tension at elevated temperatures and pressures: A molecular dynamics simulation study with biomolecular force fields, Fluid Phase Equilib. 476 (2018) 30–38. http://dx.doi.org/10.1016/i.fluid.2017.05.004.
- [29] T. Kuznetsova, B.r. Kvamme, Thermodynamic properties and interfacial tension of a model water-carbon dioxide system, Phys. Chem. Chem. Phys. 4 (6) (2002) 937–941, http://dx.doi.org/10.1039/b108726f.
- [30] J.C. Neyt, A. Wender, V. Lachet, A. Ghoufi, P. Malfreyt, Molecular modeling of the liquid-vapor interfaces of a multi-component mixture: Prediction of the coexisting densities and surface tensions at different pressures and gas compositions, J. Chem. Phys. 139 (2) (2013) http://dx.doi.org/10.1063/1. 4811679
- [31] N. Matubayasi, K. Motomura, S. Kaneshina, M. Nakamura, R. Matuura, Effect of pressure on interfacial tension between oil and water, Bull. Chem. Soc. Jpn. 50 (2) (1977) 523–524, http://dx.doi.org/10.1246/bcsj.50.523.
- [32] K. Motomura, H. Iyota, M. Aratono, M. Yamanaka, R. Matuura, Thermodynamic consideration of the pressure dependence of interfacial tension, J. Colloid Interface Sci. 93 (1) (1983) 264–269, http://dx.doi.org/10.1016/0021-9797(83) 90404-6
- [33] M. Hassan, R. Nielsen, J. Calhoun, Effect of pressure and temperature on oil-water interfacial tensions for a series of hydrocarbons, J. Pet. Technol. 5 (12) (1953) 299–306, http://dx.doi.org/10.2118/298-g.
- [34] H.Y. Jennings, G.H. Newman, Effect of temperature and pressure on the interfacial tension of water against methane- normal decane mixtures, Soc Pet. Eng J 11 (2) (1971) 171–175, http://dx.doi.org/10.2118/3071-pa.
- [35] H.Y. Jennings, The effect of temperature and pressure on the interfacial tension of benzene-water and normal decane-water, J. Colloid Interface Sci. 24 (3) (1967) 323–329, http://dx.doi.org/10.1016/0021-9797(67)90257-3.
- [36] M. Lin, J.L. Firpo, P. Mansoura, J.F. Baret, A phase transition of the adsorbed layer: High pressure effect on fatty alcohol adsorption at an oil-water interface, J. Chem. Phys. 71 (5) (1979) 2202–2206, http://dx.doi.org/10.1063/1.438551.
- [37] C.J. Lynde, Effect of pressure on surface tension, Phys. Rev. 22 (1906) 181–191, http://dx.doi.org/10.1017/CBO9781107415324.004, arXiv:arXiv:1011.1669v3.
- [38] W. Yan, G.-Y. Zhao, G.-J. Chen, T.-M. Guo, Interfacial tension of (methane + nitrogen) + water and (carbon dioxide + nitrogen) + water systems, J. Chem. Eng. Data 46 (2001) 1544–1548, http://dx.doi.org/10.1021/je0101505.
- [39] R. Massoudi, A.D. King, Effect of pressure on the surface tension of water. Adsorption of low molecular weight gases on water at 25 degrees, J. Phys. Chem. 78 (22) (1974) 2262–2266, http://dx.doi.org/10.1021/j100615a017.
- [40] C. Jho, D. Nealon, S. Shogbola, A.D. King Jr., Effect of pressure on the surface tension of water: Adsorption of hydrocarbon gases and carbon dioxide on water at temperatures between 0 and 50c, J. Colloid Interface Sci. 65 (1) (1978) 141, 154
- [41] E.J. Slowinski, E.E. Gates, C.E. Waring, The effect of pressure on the surface tensions of liquids, J. Phys. Chem. 61 (6) (1957) 808–810, http://dx.doi.org/10. 1021/j150552a028, URL http://pubs.acs.org/doi/abs/10.1021/j150552a028.
- [42] J. Satherley, D.L. Cooper, D.J. Schiffrin, Surface tension, density and composition in the methane-pentane system at high pressure, Fluid Phase Equilib. 456 (2018) 193–202, http://dx.doi.org/10.1016/j.fluid.2017.10.023.
- [43] W. Sachs, V. Meyn, Pressure and temperature dependence of the surface tension in the system natural gas/water. Principles of investigaion and the first precise experimental data for pure methane/water at 25c up to 46.8 MPa, Colloids Surfaces A Physicochem. Eng. Asp. 94 (1995) 291–301.
- [44] Q.Y. Ren, G.J. Chen, W. Yan, T.M. Guo, Interfacial tension of (CO2 + CH4) + water from 298 K to 373 K and pressures up to 30 MPa, J. Chem. Eng. Data 45 (4) (2000) 610-612, http://dx.doi.org/10.1021/je990301s.
- [45] Z.R. Hinton, N.J. Alvarez, Surface tensions at elevated pressure depend strongly on bulk phase saturation, J. Colloid Interface Sci. 594 (2021) 681–689.

- [46] M. Yamanaka, H. Iyota, M. Aratono, K. Motomura, R. Matuura, Effect of pressure on the adsorption of dodecylammonium chloride at the aqueous micellar solution/hexane interface, J. Colloid Interface Sci. 94 (2) (1983) 451–455, http://dx.doi.org/10.1016/0021-9797(83)90284-9.
- [47] M. Yamanaka, M. Aratono, K. Motomura, Effect of pressure on the adsorption and micelle formation of aqueous dodecyltrimethylammonium chloridecyclohexane system, Bull. Chem. Soc. Jpn. 59 (9) (1986) 2695–2698, http://dx.doi.org/10.1246/bcsi.59.2695.
- [48] M. Aratono, M. Yamanaka, K. Motomura, R. Matuura, Adsorption of dioctyldimethylammonium chloride at water/hexane interface, Colloid Polym. Sci. 260 (6) (1982) 632–637, http://dx.doi.org/10.1007/BF01422597.
- [49] H. Luo, Y. Zhang, W. Fan, G. Nan, Z. Li, Effects of the non-ionic surfactant (CiPOj) on the interfacial tension behavior between CO2 and crude oil, Energy Fuels 32 (2018) 6708–6712, http://dx.doi.org/10.1021/acs.energyfuels. 8b01082.
- [50] S.S. Adkins, X. Chen, Q.P. Nguyen, A.W. Sanders, K.P. Johnston, Effect of branching on the interfacial properties of nonionic hydrocarbon surfactants at the air-water and carbon dioxide-water interfaces, J. Colloid Interface Sci. 346 (2) (2010) 455–463, http://dx.doi.org/10.1016/j.jcis.2009.12.059.
- [51] S.R.P. da Rocha, K.L. Harrison, K.P.U.T.A. Johnston, Effect of surfactants on the interfacial tension and emulsion formation between water and carbon dioxide, Langmuir 15 (1999) 419–428.
- [52] T. Akutsu, Y. Yamaji, H. Yamaguchi, M. Watanabe, R.L. Smith, H. Inomata, Interfacial tension between water and high pressure CO2 in the presence of hydrocarbon surfactants, Fluid Phase Equilib. 257 (2) (2007) 163–168, http: //dx.doi.org/10.1016/j.fluid.2007.01.040.
- [53] A. Miquilena, V. Coll, A. Borges, J. Melendez, S. Zeppieri, Influence of drop growth rate and size on the interfacial tension of triton X-100 solutions as a function of pressure and temperature, Int. J. Thermophys. 31 (11–12) (2010) 2416–2424, http://dx.doi.org/10.1007/s10765-010-0825-6.
- [54] M. Sagisaka, T. Fujii, D. Koike, S. Yoda, Y. Takebayashi, T. Furuya, A. Yoshizawa, H. Sakai, M. Abe, K. Otake, Surfactant-mixing effects on the interfacial tension and the microemulsion formation in water/supercritical CO2 system, Langmuir 23 (5) (2007) 2369–2375, http://dx.doi.org/10.1021/la062789i
- [55] B. Bharatwaj, L. Wu, S.R.P. da Rocha, Biocompatible, lactide-based surfactants for the CO 2-water interface: High-pressure contact angle goniometry, tensiometry, and emulsion formation, Langmuir 23 (27) (2007) 12071–12078, http://dx.doi.org/10.1021/la701831v.
- [56] H.O. Lee, J.P. Heller, A.M. Hoefer, Change in apparent viscosity of CO2 foam with rock permeability, SPE Reserv. Eng. 6 (4) (1991) 421–428, http://dx.doi.org/10.2118/20194-PA.
- [57] F. Tewes, F. Boury, Effect of H2O CO2 organization on ovalbumin adsorption at the supercritical CO2 - water interface, J. Phys. Chem. B 109 (2005) 1874–1881.
- [58] F. Tewes, F. Boury, Dynamic and rheological properties of classic and macro-molecular surfactant at the supercritical CO2-H2O interface, J. Supercrit. Fluids 37 (2006) 375–383, http://dx.doi.org/10.1016/j.supflu.2006.02.005.
- [59] X. Chen, S.S. Adkins, Q.P. Nguyen, A.W. Sanders, K.P. Johnston, Interfacial tension and the behavior of microemulsions and macroemulsions of water and carbon dioxide with a branched hydrocarbon nonionic surfactant, J. Supercrit. Fluids 55 (2010) 712–723. http://dx.doi.org/10.1016/j.supflu.2010.08.019.
- [60] F. Tewes, M.P. Krafft, F. Boury, Dynamical and rheological properties of fluorinated surfactant films adsorbed at the pressurized CO2-H2O interface, Langmuir 27 (13) (2011) 8144–8152, http://dx.doi.org/10.1021/la201009z.
- [61] Y. Chen, A.S. Elhag, P.P. Reddy, H. Chen, L. Cui, A.J. Worthen, K. Ma, H. Quintanilla, J.A. Noguera, G.J. Hirasaki, Q.P. Nguyen, S.L. Biswal, K.P. Johnston, Phase behavior and interfacial properties of a switchable ethoxylated amine surfactant at high temperature and effects on CO2-in-water foams, J. Colloid Interface Sci. 470 (2016) 80–91, http://dx.doi.org/10.1016/j.jcis.2016.
- [62] R. Massoudi, A.D. King, Effect of pressure on the surface tension of aqueous solutions. adsorption of hydrocarbon gases, carbon dioxide, and nitrous oxide on aqueous solutions of sodium chloride and tetrabutylammonium bromide at 25.deg, J. Phys. Chem. 79 (1975) 1670–1675, http://dx.doi.org/10.1021/ i100583a012.
- [63] G.D. Bothun, Y.W. Kho, J.A. Berberich, J.P. Shofner, T. Robertson, K.J. Tatum, B.L. Knutson, Surface activity of lysozyme and dipalmitoyl phosphatidylcholine vesicles at compressed and supercritical fluid interfaces, J. Phys. Chem. B 109 (2005) 24495–24501.
- [64] J.Y. Park, J.S. Lim, C.H. Yoon, C.H. Lee, K.P. Park, Effect of a fluorinated sodium bis(2-ethylhexyl) sulfosuccinate (aerosol-OT, AOT) analogue surfactant on the interfacial tension of CO 2 + water and CO2 + Ni-plating solution in near- and supercritical CO2, J. Chem. Eng. Data 50 (2) (2005) 299–308, http://dx.doi.org/10.1021/je0499667.
- [65] J. Liu, B. Han, Z. Wang, J. Zhang, G. Li, G. Yang, Solubility of ls-36 and ls-45 surfactants in supercritical CO2 and loading water in the CO2/water/surfactant systems, Langmuir 18 (8) (2002) 3086–3089, http://dx.doi.org/10.1021/la011721u.

- [66] W. Yu, D. Zhou, J.Z. Yin, J.J. Gao, Phase behavior of supercritical CO2 microemulsions with surfactant ls-36 and selective solubilization of propane-1,3-diol, J. Chem. Eng. Data 58 (3) (2013) 814–820, http://dx.doi.org/10.1021/je301356r.
- [67] V. Nace (Ed.), Nonionic Surfactants: Polyoxyalkylene Block Copolymers, CRC Press, Boca Raton, FL, 2019.
- [68] M. Schwarze, J.S. Milano-Brusco, V. Strempel, T. Hamerla, S. Wille, C. Fischer, W. Baumann, W. Arlt, R. Schomäcker, Rhodium catalyzed hydrogenation reactions in aqueous micellar systems as green solvents, RSC Adv. 1 (3) (2011) 474–483, http://dx.doi.org/10.1039/c1ra00397f.
- [69] M. Sato, A. Quye, Detergency evaluation of non-ionic surfactant dehypon LS54 for textile conservation wet cleaning, J. Inst. Conserv. 42 (1) (2019) 3–17, http://dx.doi.org/10.1080/19455224.2018.1556719.
- [70] A.L. Fricker, D.S. McPhail, B. Keneghan, B. Pretzel, Investigating the impact of cleaning treatments on polystyrene using SEM, AFM and tof-SIMS, Herit. Sci. 5 (1) (2017) 1–9, http://dx.doi.org/10.1186/s40494-017-0142-5.
- [71] J. Tsibouklis, M.J. Stone, R.E. Avery, Hard surface cleaners containing ethylene oxide/propylene oxide block copolymer surfactants, ISBN: 1020100095, 2004.
- [72] M. Milosevic, K.J. Staal, G. Bargeman, B. Schuur, A.B. De Haan, Fractionation of aqueous sodium salts by liquid-liquid extraction in aqueous two phase systems, Sep. Purif. Technol. 125 (2014) 208–215, http://dx.doi.org/10.1016/j.seppur. 2014.01.058.
- [73] M. Milosevic, K.J. Staal, B. Schuur, A.B. De Haan, Liquid-liquid phase equilibria for ternary systems of several polyethers with NaCl and H2O, Fluid Phase Equilib. 376 (2014) 76–84, http://dx.doi.org/10.1016/j.fluid.2014.05.027.
- [74] F.A.A. Mutalib, J.M. Jahim, F.D.A. Bakar, A.W. Mohammad, O. Hassan, Characterisation of new aqueous two-phase systems comprising of dehypon LS54 and K4484 dextrin for potential cutinase recovery, Sep. Purif. Technol. 123 (2014) 183–189, http://dx.doi.org/10.1016/j.seppur.2013.12.037.
- [75] K.a. Consan, R.D. Smith, Observations on the solubility of surfactants and related molecules in carbon dioxide at 50 degrees C, J. Supercrit. Fluids 3 (2) (1990) 51–65, http://dx.doi.org/10.1016/0896-8446(90)90008-A.
- [76] M.T. Stone, P.G. Smith, S.R.P. da Rocha, P.J. Rossky, K.P. Johnston, Low interfacial free volume of stubby surfactants stabilizes water-in-carbon dioxide microemulsions, J. Phys. Chem. B 108 (6) (2004) 1962–1966, http://dx.doi. org/10.1021/jp036224w.
- [77] J. Eastoe, S. Gold, D.C. Steytler, Surfactants for CO2, Langmuir 22 (6) (2006) 9832–9842.
- [78] M.A. Matthews, J.M. Becnel, Diffusion coefficients of methyl orange in dense carbon dioxide with the micelle-forming surfactant dehypon Ls-54, J. Chem. Eng. Data 48 (6) (2003) 1413–1417, http://dx.doi.org/10.1021/je020211e.
- [79] Y. Gao, Z. Wang, W. Hou, G. Li, B. Han, G. Zhang, Studies on dynamic surface tension of an outstanding microemulsifier in supercritical CO2 and its wetting performance, J. Dispers. Sci. Technol. 26 (6) (2005) 745–751, http://dx.doi.org/10.1081/DIS-200063069.
- [80] Y. Gao, S. Wang, L. Zheng, G. Li, W. Hou, X. Zhang, D. Lu, S. Zhang, G. Zhang, Q. Huang, Study on the dynamic surface tension of nonionic surfactant LS45 and LS54 solutions, J. Dispers. Sci. Technol. 28 (1) (2007) 181–187, http://dx.doi.org/10.1080/01932690601028664.
- [81] T. Fenton, K. Kanyuck, T. Mills, E. Pelan, Formulation and characterisation of kappa-carrageenan gels with non-ionic surfactant for melting-triggered controlled release, Carbohydrate Poly. Tech. Appl. 2 (2021) 100060.
- [82] Z.R. Hinton, N.J. Alvarez, A molecular parameter to scale the gibbs free energies of adsorption and micellization for nonionic surfactants, Colloids Surf., A 609 (2021) 125622
- [83] N.J. Alvarez, L.M. Walker, S.L. Anna, A microtensiometer to probe the effect of radius of curvature on surfactant transport to a spherical interface, Langmuir 26 (10) (2010) 13310–13319, http://dx.doi.org/10.1021/la101870m.
- [84] N.J. Alvarez, L.M. Walker, S.L. Anna, A criterion to assess the impact of confined volumes on surfactant transport to liquid-fluid interfaces, Soft Matter 8 (34) (2012) 8917, http://dx.doi.org/10.1039/c2sm25447f.
- [85] C. Yang, Y. Gu, Modeling of the adsorption kinetics of surfactants at the liquid-fluid interface of a pendant drop, Langmuir 20 (6) (2004) 2503–2511, http://dx.doi.org/10.1021/la0360097.
- [86] Z.R. Hinton, N.J. Alvarez, Accounting for optical errors in microtensiometry, J. Colloid Interface Sci. 526 (2018) 392–399, http://dx.doi.org/10.1016/j.jcis. 2018.04.053.
- [87] Z.R. Hinton, The role of chemistry and pressure on surfactant interfacial thermodynamics (Ph.D. thesis), Drexel University, 2020.
- [88] K. Yasuda, Y.H. Mori, R. Ohmura, Interfacial tension measurements in water-methane system at temperatures from 278.15 k to 298.15 k and pressures up to 10 MPa, Fluid Phase Equilib. 413 (2016) 170–175, http://dx.doi.org/10.1016/j.fluid.2015.10.006.

- [89] A.W. Adamson, A.P. Gast, Physical Chemistry of Surfaces, 6th, Wiley-Interscience, New York, 1997.
- [90] A.M. Prpich, M. Elias Biswas, P. Chen, Adsorption kinetics of aqueous nalcohols: A new kinetic equation for surfactant transfer, J. Phys. Chem. C 112 (7) (2008) 2522–2528, http://dx.doi.org/10.1021/jp077012s.
- [91] V.S. Chernyshev, M. Skliar, Surface tension of water in the presence of perfluorocarbon vapors, Soft Matter 10 (12) (2014) 1937–1943, http://dx.doi. org/10.1039/c3sm52289i.
- [92] M.J. Rosen, Surfactants and Interfacial Phenomena, fourth ed., John Wiley & Sons, Hoboken, N.J. 2004, http://dx.doi.org/10.1016/0166-6622(89)80030-7.
- [93] Z.R. Hinton, N.J. Alvarez, Effects of constituent block size on the interfacial dynamics of Ci(EO)n(PO)m block copolymer surfactants, in: Proc. Am. Chem. Soc. 252nd Natl. Meet., Philadelphia, PA, 2016.
- [94] Z.R. Hinton, N.J. Alvarez, A unified structure-property relationship for alkyl-polyoxide surfactants, in: Proc. Am. Inst. Chem. Eng. Annu. Meet., Minneapolis, MN, 2017.
- [95] P. Bauduin, L. Wattebled, D. Touraud, W. Kunz, Hofmeister ion effects on the phase diagrams of water-propylene glycol propyl ethers, Z. Phys. Chem. 218 (6) (2004) 631–641, http://dx.doi.org/10.1524/zpch.218.6.631.33453.
- [96] J. Eastoe, J.S. Dalton, Dynamic surface tension and adsorption mechanisms of surfactants at the air-water interface, Adv. Colloid Interface Sci. 85 (2) (2000) 103–144, http://dx.doi.org/10.1016/S0001-8686(99)00017-2.
- [97] A.P. Kotula, S.L. Anna, Regular perturbation analysis of small amplitude oscillatory dilatation of an interface in a capillary pressure tensiometer, J. Rheol. (N. Y. N. Y). 59 (1) (2015) 85–117, http://dx.doi.org/10.1122/1.4902546.
- [98] C. Peng, J.P. Crawshaw, G.C. Maitland, J.P. Martin Trusler, D. Vega-Maza, The pH of CO2-saturated water at temperatures between 308 k and 423 k at pressures up to 15 MPa, J. Supercrit. Fluids 82 (2013) 129–137, http://dx.doi.org/10.1016/j.supflu.2013.07.001.
- [99] J.R. Bloor, J.C. Morrison, C.T. Rhodes, Effect of pH on the micellar properties of a nonionic surfactant, J. Pharm. Sci. 59 (3) (1970) 387–391, http://dx.doi. org/10.1001/jama.195.11.943.
- [100] T. Zhou, H. Yang, X. Xu, X. Wang, J. Wang, G. Dong, Synthesis, surface and aggregation properties of nonionic poly(ethylene oxide) gemini surfactants, Colloids Surfaces A Physicochem. Eng. Asp. 317 (1–3) (2008) 339–343, http: //dx.doi.org/10.1016/j.colsurfa.2007.11.008.
- [101] M.S. Hossain, S. Berg, C.A.S. Bergström, P. Larsson, Aggregation behavior of medium chain fatty acids studied by coarse-grained molecular dynamics simulation, AAPS PharmSciTech 20 (2019) 61.
- [102] M. Lesemann, K. Thirumoorthy, Y.J. Kim, J. Jonas, M.E. Paulaitis, Pressure dependence of the critical micelle concentration of a nonionic surfactant in water studied by 1H-NMR, Langmuir 14 (19) (1998) 5339–5341, http://dx.doi. org/10.1021/la9805692.
- [103] K. Hara, H. Kuwabara, Effect of pressure on the critical micelle concentration of neutral surfactant using fluorescence probe method, J. Photochem. Photobiol. A 124 (1999) 159–162, URL http://www.sciencedirect.com/science/article/pii/ S1010603099000635.
- [104] R. Alvares, S. Gupta, P.M. Macdonald, R.S. Prosser, Temperature and pressure based NMR studies of detergent micelle phase equilibria, J. Phys. Chem. B 118 (21) (2014) 5698–5706, http://dx.doi.org/10.1021/jp500139p.
- [105] Y.R. Espinosa Silva, J.R. Grigera, Micelle stability in water under a range of pressures and temperatures; do both have a common mechanism? RSC Adv. 5 (86) (2015) 70005–70009, http://dx.doi.org/10.1039/c5ra09377e.
- [106] J. Chen, J. Zhang, B. Han, X. Feng, M. Hou, W. Li, Z. Zhang, Effect of compressed CO2 on the critical micelle concentration and aggregation number of AOT reverse micelles in isooctane, Chem. - A Eur. J. 12 (31) (2006) 8067–8074, http://dx.doi.org/10.1002/chem.200501593.
- [107] N.J. Alvarez, L.M. Walker, S.L. Anna, A non-gradient based algorithm for the determination of surface tension from a pendant drop: application to low bond number drop shapes, J. Colloid Interface Sci. 333 (2) (2009) 557–562.
- [108] N.J. Alvarez, L.M. Walker, S.L. Anna, Diffusion-limited adsorption to a spherical geometry: The impact of curvature and competitive time scales, Phys. Rev. E - Stat. Nonlinear, Soft Matter Phys. 82 (1) (2010) 1–8, http://dx.doi.org/10. 1103/PhysRevE.82.011604.
- [109] M. Martin, G. Guiochon, Pressure dependence of diffusion coefficient and effect on plate height in liquid chromatography, Anal. Chem. 55 (14) (1983) 2302–2309.
- [110] J. Lyklema, Fundamentals of Interface and Colloid Science: Volume III Liquid-Fluid Interfaces, Academic Press, San Diego, 2000.